

Deep Learning for Joint Design of Pilot, Channel Feedback, and Hybrid Beamforming in FDD Massive MIMO-OFDM Systems

Junyi Yang, Weifeng Zhu, Shu Sun, Xiaofeng Li, Xingqin Lin, and Meixia Tao

Abstract—This letter considers the transceiver design in frequency division duplex (FDD) massive multiple-input multiple-output (MIMO) orthogonal frequency division multiplexing (OFDM) systems for high-quality data transmission. We propose a novel deep learning based framework where the procedures of pilot design, channel feedback, and hybrid beamforming are realized by carefully crafted deep neural networks. All the considered modules are jointly learned in an end-to-end manner, and a graph neural network is adopted to effectively capture interactions between beamformers based on the built graphical representation. Numerical results validate the effectiveness of our method.

Index Terms—Hybrid beamforming, limited feedback, deep learning, graph neural network.

I. INTRODUCTION

Massive multiple-input multiple-output (MIMO) is an essential technology in the fifth generation (5G) wireless systems and beyond, owing to its remarkable capacity of beamforming towards desired directions thus significantly enhancing spectral efficiency [1]. Massive MIMO beamforming requires the knowledge of downlink channel state information (CSI) at the base station (BS). In time-division duplex (TDD) systems, downlink CSI can be estimated directly at the BS based on uplink transmission by channel reciprocity. In contrast, in frequency-division duplex (FDD) systems, downlink CSI acquisition typically requires the user equipment (UE) to channel estimation based on downlink pilot transmission and then feedback the CSI to the BS. Considering the signaling overhead and computational complexity, the pilot design, channel estimation, feedback mechanism, and beamforming design constitute the primary challenges for implementing massive MIMO beamforming in FDD systems.

Recently, thanks to the powerful deep learning (DL) techniques, many studies have proposed using deep neural networks to design the aforementioned modules, namely, pilot

transmission, CSI estimation and feedback, and beamforming, in FDD massive MIMO systems either separately or jointly [2]–[10]. In particular, in works [2]–[4], only one of the modules is individually optimized using DL techniques. More specifically, the work [2] introduces a DNN called CsiNet for CSI feedback, while works [3], [4] utilize DNNs comprised of fully-connected and convolutional layers for beamforming design. To further enhance performance, works [5]–[8] propose the DL-based method for the joint design of CSI feedback and beamforming. Therein, works [5], [6] consider beamforming design based on channels estimated by conventional methods, while works [7], [8] assume perfect CSI at the receiver. In works [9], [10], the pilot design, CSI feedback and beamforming are jointly optimized by DL techniques. Note that these works on joint design [9], [10] only focus on fully digital beamforming, which requires each antenna to be connected to a dedicated RF chain, yielding potentially unaffordable hardware costs and increased power consumption [11]. In addition, the aforementioned works [2]–[10] only consider narrowband systems. Directly extending these methods to broadband systems can result in a substantial increase in the number of trainable parameters.

This letter considers the practical FDD broadband massive MIMO systems with orthogonal frequency division multiplexing (OFDM) modulation and hybrid analog-digital beamforming architecture. We propose a novel DL framework to realize the joint design of pilot transmission, channel feedback, and hybrid beamforming. The main distinctions and contributions of this work in comparison to the existing literature are as follows. First, our considered FDD massive MIMO system is more practical with OFDM-based broadband transmission using hybrid analog-digital beamforming architecture. Therein, each subchannel consists of a set of subcarriers and is associated with an individual digital beamformer, and all subchannels share a common analog beamformer. Second, our DL-based joint design utilizes learned pilot signals and a paired vector quantized variational auto-encoder (VQ-VAE) for channel estimation and feedback. Compared to conventional compression-reconstruction-based channel feedback methods, VQ-VAE can represent the discrete characteristics of the received signal space more accurately, thus facilitating the efficient collection and feedback of channel information. Third, a novel graph neural network (GNN) is proposed for hybrid beamforming and combining (HBC) design based on the channel information feedback. The proposed GNN can effectively capture the interactions between the analog and dig-

(Corresponding authors: Meixia Tao; Shu Sun.)

J. Yang, S. Sun, and M. Tao are with the Department of Electronic Engineering and the Cooperative Medianet Innovation Center (CMIC), Shanghai Jiao Tong University, Shanghai, 200240, China (emails: {yangjunyi, shusun, mxtao}@sjtu.edu.cn)

W. Zhu is with the Department of Electrical and Electronic Engineering, The Hong Kong Polytechnic University, Hong Kong, SAR, China (e-mail: eee-wf.zhu@polyu.edu.hk)

X. Li is with Intel Corporation, Santa Clara, CA, USA (email: xiaofeng.li@intel.com)

X. Lin is with Nvidia Corporation, Santa Clara, CA, USA (email: xingqinl@nvidia.com)

ital beamformers in broadband systems, leading to significant performance improvements. Numerical results demonstrate that our method can consistently achieve a 16%~21% higher spectral efficiency comparing to existing alternatives under the same pilot length and closely approach the performance of the benchmark system with the fully digital architecture and unlimited channel feedback capacity.

II. SYSTEM MODEL AND PROBLEM FORMULATION

We consider an FDD MIMO-OFDM system, where an N_t -antenna BS with $N_{\text{RF},t}$ RF chains serves an N_r -antenna UE with $N_{\text{RF},r}$ RF chains and N_s parallel data streams $\mathbf{s}[k] \in \mathbb{C}^{N_s \times 1}$ over K subchannels. Here, we have $N_t > N_{\text{RF},t} \geq N_s$, $N_r > N_{\text{RF},r} \geq N_s$. Let $\mathcal{K} = \{1, 2, \dots, K\}$ denote the set of subchannels.

The whole communication procedure between the BS and UE involves three stages of pilot transmission, channel feedback and data transmission. First, in the pilot transmission stage, the BS transmits pilots to the UE over K_p uniformly-spaced subchannels. Let $\mathcal{K}_p = \{1, M+1, \dots, (K_p-1)M+1\} \in \mathcal{K}$ denote the subchannel set for pilot transmission, where M represents the subchannel interval. We assume that the pilot length is L and each pilot vector, denoted as $\tilde{\mathbf{s}}_l \in \mathbb{C}^{N_{\text{RF},t} \times 1}$ is subject to the power constraint $\|\tilde{\mathbf{s}}_l\|_2^2 \leq N_{\text{RF},t}$. Let $\mathcal{L} = \{1, 2, \dots, L\}$ denote the set of pilot indices. Then the l -th received pilot signal at the k_p -th subchannel can be expressed as

$$\tilde{\mathbf{y}}_l[k_p] = \sqrt{\rho_p} \tilde{\mathbf{W}}_{\text{RF},l}^H \mathbf{H}[k_p] \tilde{\mathbf{F}}_{\text{RF},l} \tilde{\mathbf{s}}_l + \tilde{\mathbf{W}}_{\text{RF},l}^H \tilde{\mathbf{n}}_l[k_p], \quad \forall l \in \mathcal{L}, k_p \in \mathcal{K}_p, \quad (1)$$

where $\tilde{\mathbf{y}}_l[k_p]$ denotes the l -th column of the received pilot matrix $\tilde{\mathbf{Y}}[k_p]$, $\mathbf{H}[k_p] \in \mathbb{C}^{N_r \times N_t}$ denotes the frequency-domain channel matrix at the k_p -th subchannel, ρ_p is the power for pilot transmission, $\tilde{\mathbf{n}}_l[k_p] \sim \mathcal{CN}(0, \sigma_n^2 \mathbf{I}_{N_r})$ indicates the k_p -th subchannel noise vectors at the l -th pilot transmission. $\tilde{\mathbf{F}}_{\text{RF},l} \in \mathbb{C}^{N_t \times N_{\text{RF},t}}$ and $\tilde{\mathbf{W}}_{\text{RF},l} \in \mathbb{C}^{N_r \times N_{\text{RF},r}}$ represent the analog beamformer and combiner in the l -th pilot transmission, respectively, which follow the constant modulus constraints $\|[\tilde{\mathbf{F}}_{\text{RF},l}]_{i,j}\|^2 = \frac{1}{N_t}$ and $\|[\tilde{\mathbf{W}}_{\text{RF},l}]_{i,j}\|^2 = \frac{1}{N_r}$.

After the pilot transmission, the received pilot signals $\mathcal{R} = \{\tilde{\mathbf{Y}}[k_p]\}_{k_p \in \mathcal{K}_p}$ are encoded into a bit stream of length B by a feedback encoder, denoted as $\mathbf{q} = v_e(\mathcal{R}) \in \{0, 1\}^{B \times 1}$. This bit stream is then assumed to be fed back to the BS error free. With the feedback \mathbf{q} , the BS recovers the received signals by a feedback decoder as $\hat{\mathcal{R}} = v_d(\mathbf{q})$, and then designs the hybrid beamformer $\mathcal{F} = \{\mathbf{F}_{\text{RF}}, \{\mathbf{F}_{\text{BB}}[k]\}_{k \in \mathcal{K}}\}$ with $\hat{\mathcal{R}}$. Here, we denote the recovered signals as $\hat{\mathcal{R}} = \{\tilde{\mathbf{Y}}[k_p]\}_{k_p \in \mathcal{K}_p}$. For the UE, the hybrid combiner $\mathcal{W} = \{\mathbf{W}_{\text{RF}}, \{\mathbf{W}_{\text{BB}}[k]\}_{k \in \mathcal{K}}\}$ can be designed based on its received pilot signals \mathcal{R} . Here, $\mathbf{F}_{\text{RF}} \in \mathbb{C}^{N_t \times N_{\text{RF},t}}$ and $\mathbf{W}_{\text{RF}} \in \mathbb{C}^{N_r \times N_{\text{RF},r}}$ represent the analog beamformer and combiner at the BS and the UE, respectively, which also follow the constant modulus constraints $\|[\mathbf{F}_{\text{RF}}]_{i,j}\|^2 = \frac{1}{N_t}$ and $\|[\mathbf{W}_{\text{RF}}]_{i,j}\|^2 = \frac{1}{N_r}$; $\mathbf{F}_{\text{BB}}[k] \in \mathbb{C}^{N_{\text{RF},t} \times N_s}$ and $\mathbf{W}_{\text{BB}}[k] \in \mathbb{C}^{N_{\text{RF},r} \times N_s}$ represent the digital beamformer and combiner at the k -th subchannel, respectively. We also consider the power constraint for the hybrid analog and digital beamformers, i.e., $\sum_{k=1}^K \|\mathbf{F}_{\text{RF}} \mathbf{F}_{\text{BB}}[k]\|_F^2 = KN_s$. Note that we propose to directly process \mathcal{R} without explicitly

reconstructing the channel matrix throughout the process (i.e., implicit channel estimation), which is potential to greatly reduce the signaling overhead and thus further improve the system performance. The hybrid beamformer and combiner design can be modeled as:

$$\mathcal{F} = f(\hat{\mathcal{R}}), \quad (2)$$

$$\mathcal{W} = g(\mathcal{R}). \quad (3)$$

Finally, we adopt the fully-connected hybrid beamforming architecture at both the BS and UE for downlink data transmission, where all the subchannels share the common analog beamformer \mathbf{F}_{RF} at the BS (and the common analog combiner \mathbf{W}_{RF} at the UE), while each subchannel has its own individual digital beamformer $\mathbf{F}_{\text{BB}}[k]$ (and digital combiner $\mathbf{W}_{\text{BB}}[k]$) for $k \in \mathcal{K}$. Then the received signal of the k -th subchannel is given by

$$\mathbf{y}[k] = \sqrt{\rho} \mathbf{W}_{\text{BB}}^H[k] \mathbf{W}_{\text{RF}}^H \mathbf{H}[k] \mathbf{F}_{\text{RF}} \mathbf{F}_{\text{BB}}[k] \mathbf{s}[k] + \mathbf{W}_{\text{BB}}^H[k] \mathbf{W}_{\text{RF}}^H \mathbf{n}[k], \quad \forall k \in \mathcal{K}. \quad (4)$$

where ρ and $\mathbf{n}[k] \sim \mathcal{CN}(0, \sigma_n^2 \mathbf{I}_{N_r})$ denote the transmit power and noise vector, $\mathbf{s}[k] \in \mathbb{C}^{N_s \times 1}$ is the information symbol which satisfies the constraint $\mathbb{E}\{\mathbf{s}[k] \mathbf{s}^H[k]\} = \mathbf{I}_{N_s}$. The spectral efficiency of the system can be computed as

$$R = \frac{1}{K} \sum_{k \in \mathcal{K}} \log \det \left(\mathbf{I}_{N_s} + \frac{\rho}{N_s} \boldsymbol{\Omega}^{-1}[k] \boldsymbol{\Lambda}[k] \boldsymbol{\Lambda}^H[k] \right), \quad (5)$$

where $\boldsymbol{\Omega}[k] = \sigma_n^2 \mathbf{W}_{\text{BB}}^H[k] \mathbf{W}_{\text{RF}}^H \mathbf{W}_{\text{RF}} \mathbf{W}_{\text{BB}}[k] \in \mathbb{C}^{N_s \times N_s}$ and $\boldsymbol{\Lambda}[k] = \mathbf{W}_{\text{BB}}^H[k] \mathbf{W}_{\text{RF}}^H \mathbf{H}[k] \mathbf{F}_{\text{RF}} \mathbf{F}_{\text{BB}}[k] \in \mathbb{C}^{N_s \times N_s}$.

Based upon the above signal processing procedure, we jointly design the pilot parameter $\mathcal{P} = \{\tilde{\mathbf{W}}_{\text{RF},l}, \tilde{\mathbf{F}}_{\text{RF},l}, \tilde{\mathbf{s}}_l\}_{l=1}^L$, the feedback, and the hybrid beamforming to maximize the spectral efficiency in the massive MIMO-OFDM system. The optimization problem can be formulated as

$$\max_{\substack{\mathcal{P}, v_e(\cdot), v_d(\cdot), \\ \mathcal{F}, \mathcal{W}, f(\cdot), g(\cdot)}} R \quad \text{in (5)} \quad (6a)$$

$$\text{s.t.} \quad \|[\mathbf{F}_{\text{RF}}]_{i,j}\|^2 = \|[\tilde{\mathbf{F}}_{\text{RF},l}]_{i,j}\|^2 = \frac{1}{N_t}, \quad \forall i, j, \quad (6b)$$

$$\|[\mathbf{W}_{\text{RF}}]_{i,j}\|^2 = \|[\tilde{\mathbf{W}}_{\text{RF},l}]_{i,j}\|^2 = \frac{1}{N_r}, \quad \forall i, j, \quad (6c)$$

$$\sum_{k=1}^K \|\mathbf{F}_{\text{RF}} \mathbf{F}_{\text{BB}}[k]\|_F^2 = KN_s, \quad (6d)$$

$$\|\tilde{\mathbf{s}}_l\|_2^2 \leq N_{\text{RF},t}, \quad \forall l, \quad (6e)$$

$$\mathbf{q} = v_e(\mathcal{R}), \quad \hat{\mathcal{R}} = v_d(\mathbf{q}), \quad (6f)$$

$$(1), (2), (3). \quad (6g)$$

The above optimization problem contains both variable optimization and function optimization. To tackle this challenging problem, we propose a DL-based approach to learn the pilot parameter \mathcal{P} and to parameterize the mapping functions $v_e(\cdot)$, $v_d(\cdot)$, $f(\cdot)$ and $g(\cdot)$ by deep neural networks, whose details will be given in the next section.

III. PROPOSED DL-BASED METHOD

In this section, we propose a DL-based method to acquire the hybrid beamformer in the FDD massive MIMO-OFDM system. As illustrated in Fig. 1, the proposed DL architecture consists of a pilot network (PN), a feedback network (FN),

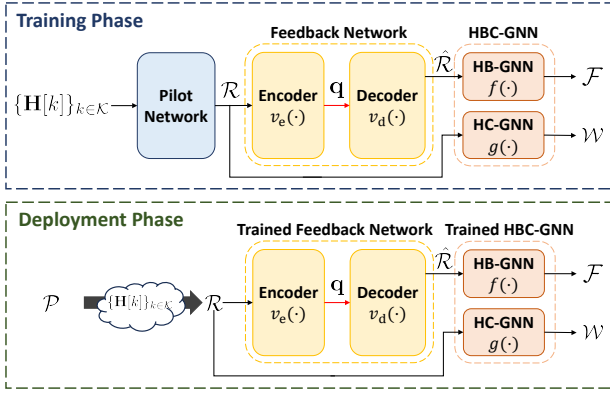


Fig. 1. The diagram of the proposed DL-based method.

and an HBC-GNN. The parameters in these DNNs are jointly optimized during the training phase before deployment.

A. Pilot Network

The PN is trained to obtain the pilot parameter \mathcal{P} for channel estimation. Due to the constant-modulus constraint on each element in $\tilde{\mathbf{F}}_{\text{RF},l}$ and $\tilde{\mathbf{W}}_{\text{RF},l}$ (6b)(6c), the PN obtains the phase shifts of them, which satisfy the equation:

$$\tilde{\mathbf{F}}_{\text{RF},l} = \frac{1}{\sqrt{N_t}} \left[\cos(\tilde{\Theta}_l) + j \cdot \sin(\tilde{\Theta}_l) \right], \quad (7a)$$

$$\tilde{\mathbf{W}}_{\text{RF},l} = \frac{1}{\sqrt{N_r}} \left[\cos(\tilde{\Phi}_l) + j \cdot \sin(\tilde{\Phi}_l) \right], \quad (7b)$$

where $\tilde{\Theta}_l \in \mathbb{R}^{N_t \times N_{\text{RF},t}}$ and $\tilde{\Phi}_l \in \mathbb{R}^{N_r \times N_{\text{RF},r}}$ represent the matrices of phase shifts at the BS and the UE, respectively. Thus we consider $\{\tilde{\Theta}_l, \tilde{\Phi}_l, \tilde{s}_l\}_{l=1}^L$ as the trainable variables and (1) can be regarded as a forward-pass computation of $\mathbf{H}[k_p]$ through a two-layer network. Once the training of the PN is completed, we will directly use the trained \mathcal{P} to acquire the channel information in the deployment phase.

B. Feedback Network

Based on the signal processing procedure in Section III, we can follow the auto-encoder neural network architecture to design the FN. In this work, we adopt the VQ-VAE neural network [12] for feedback by exploiting its high-quality compression ability. The key idea of VQ-VAE is to train a codebook that can accurately characterize the discrete representation of the input signal space. The pilot signal \mathcal{R} is first split to several vectors, then VQ-VAE utilizes the codeword closest to each vector from the trained codebook as its output. In our work, the trained codebook is pre-stored at both the UE and the BS, while the binary vector \mathbf{q} in the feedback link in fact represents the indices of the selected codewords by the encoder. For illustration, we denote the loss function of VQ-VAE as \mathcal{L}_V , which can be regarded as the mean squared error (MSE) between the received pilot signals and the selected codewords by the encoder.

C. Hybrid Beamforming and Combining Graph Neural Network

To better exploit the interactions between the analog beamformer and digital beamformers, we utilize the GNN for hybrid

beamforming design. In the MIMO-OFDM system, there is a particular digital beamformer for each subchannel, while the analog beamformer is shared among all the subchannels. Compared with the fully-connected neural network, GNN can naturally embed the topological relations in its network architecture and thus enjoys permutation invariance and permutation equivariance of the optimization problem (6). Here, permutation invariance means that the analog beamformer \mathbf{F}_{RF} is independent of the ordering of the subchannels, while permutation equivariance means that the $\{\mathbf{F}_{\text{BB}}[k]\}_{k \in \mathcal{K}}$ will be permuted in the same way if the subchannels are permuted. Furthermore, the reduced model complexity and improved generalization performance also make the GNN more favorable.

Before the GNN design, we build the graphical representation of \mathbf{F}_{RF} and $\{\mathbf{F}_{\text{BB}}[k]\}_{k \in \mathcal{K}}$ at the BS. As shown in Fig. 2(a), the analog beamformer \mathbf{F}_{RF} is represented by the circular node and the digital beamformers $\{\mathbf{F}_{\text{BB}}[k]\}_{k \in \mathcal{K}}$ are presented by square nodes. There is an associated state vector $\mathbf{c}_k \in \mathbb{R}^{2N_{\text{RF},t} \times 1}$ and $\mathbf{v} \in \mathbb{R}^{2N_{\text{RF},t} \times 1}$ for each digital beamformer node and analog beamformer node, respectively. These vectors will be updated layer by layer in the GNN to collect sufficient useful information, and finally yield the beamformers of their corresponding nodes. Note that the graphical representation of \mathbf{W}_{RF} and $\{\mathbf{W}_{\text{BB}}[k]\}_{k \in \mathcal{K}}$ at the UE can be established in a similar way.

Based on the graphical representation, we propose a HBC-GNN which contains a hybrid beamforming GNN (HB-GNN) and a hybrid combining GNN (HC-GNN) to obtain \mathcal{F} and \mathcal{W} , respectively. The HB-GNN and HC-GNN have similar network structures, thus we only provide the details of the HB-GNN below. The architecture of the proposed HB-GNN architecture is shown in Fig.2(b), which consists of the following three parts.

1) *Initialization Layer*: This layer consists of two DNNs to obtain the initialization for all nodes. Considering the correlation between adjacent subchannels, we initialize the digital beamformer node for each subchannel based on the collected channel information from its nearby pilot-bearing subchannels. Specifically, all digital beamformer nodes are divided into K_p groups and the multilayer perceptron (MLP) $I_{\text{BB}}(\cdot)$ is designed for all groups to generate initial state vectors as $\{\mathbf{c}_{k_p}^0, \mathbf{c}_{k_p+1}^0, \dots, \mathbf{c}_{k_p+M-1}^0\} = I_{\text{BB}}(\hat{\mathbf{Y}}[k_p])$, $k_p \in \mathcal{K}_p$. For the analog beamformer node, the state vector is initialized by the MLP $I_{\text{RF}}(\cdot)$ as $\mathbf{v}^0 = I_{\text{RF}}(\bar{\mathbf{Y}})$, where $\bar{\mathbf{Y}} = \psi(\{\hat{\mathbf{Y}}[k_p]\}_{k_p \in \mathcal{K}_p})$ and $\psi(\cdot)$ adopts the element-wise mean function due to the fact that each digital beamformer node has equal contribution to the analog beamformer node. Note that such a property is also utilized in the design of the following aggregation and combination layers.

2) *G Layers of Aggregation and Combination*: In the g -th aggregation and combination layer, the state vector of each node is updated by combining its own state vector and the aggregation of state vectors from its neighbor nodes.

Specifically, in the g -th aggregation and combination layer, the state vector of the analog beamformer node is updated as

$$\mathbf{v}^g = f_1^g(\mathbf{v}^{g-1}) + f_2^g(\bar{\mathbf{c}}^{g-1}), \quad (8)$$

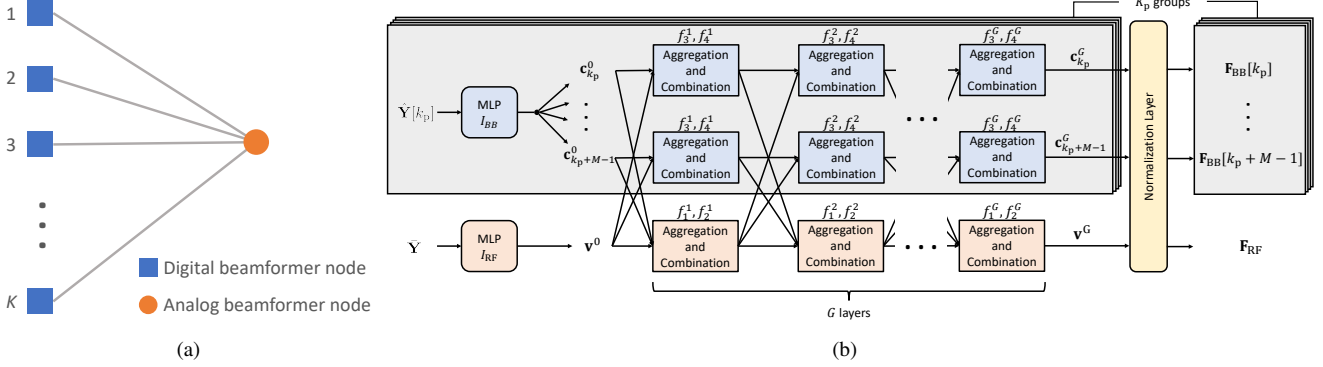


Fig. 2. (a) Graphical representation of the hybrid beamformer at the BS; (b) The network architecture of the proposed HB-GNN.

where $\bar{\mathbf{c}}^{g-1} = \psi(\{\mathbf{c}_k^{g-1}\}_{k \in \mathcal{K}})$, $f_1^g(\cdot)$ and $f_2^g(\cdot)$ are realized by MLPs. For digital beamformer nodes, the state vector of digital beamformer node k in the g -th layer can be given by

$$\mathbf{c}_k^g = f_3^g(\mathbf{c}_k^{g-1}) + f_4^g(\mathbf{v}^{g-1}), \quad \forall k \in \mathcal{K}, \quad (9)$$

where $f_3^g(\cdot)$ and $f_4^g(\cdot)$ also employ MLPs and they are reused in K_p groups just like $I_{BB}(\cdot)$.

3) *Normalization Layer*: After G -layer aggregation and combination, we obtain the hybrid beamformers from the state vectors $\{\mathbf{c}_k^G\}_{k=1}^K$ and \mathbf{v}^G . Here, each state vector exactly consists of the real and imaginary components of its corresponding beamformer and can be represented as

$$\mathbf{v}^G = \text{vec}([\Re\{\mathbf{F}_{RF}\}, \Im\{\mathbf{F}_{RF}\}]), \quad (10)$$

$$\mathbf{c}_k^G = \text{vec}([\Re\{\mathbf{F}_{BB}[k]\}, \Im\{\mathbf{F}_{BB}[k]\}]), \quad \forall k \in \mathcal{K}, \quad (11)$$

Then, a normalization layer is utilized to scale $\{\mathbf{F}_{BB}[k]\}_{k \in \mathcal{K}}$ and each element in \mathbf{F}_{RF} , which ensures that the constraints (6b), (6c), and (6d) are satisfied.

In practice, each MLP in the proposed HB-GNN and HC-GNN is modeled as only one fully-connected layer with an activation function, and the input/output dimension is determined based on the input/output vector.

D. Network Training

We adopt the end-to-end training strategy to train the proposed pilot network, VQ-VAE, HB-GNN, and HC-GNN jointly. The loss function is defined as

$$\mathcal{L} = \alpha \mathcal{L}_V - R \quad (12)$$

where α is the weight factor keeping fixed during the training phase and the optimal value of α can be obtained by empirical results. The first term of (12) corresponds to supervised learning for implicit CSI transmission, which ensures that the received pilot signals and the codewords in the VQ-VAE have similar distributions. The second term of (12) pertains to unsupervised learning for maximizing the transmission rate. In the training phase, we only need to collect channel samples in a targeted environment which serve as the input to the proposed neural network, without the need of creating labels. Note that the proposed DNN is site-specific and needs to be retrained if the channel statistics vary. In practice, the channel statistics usually evolve slowly and remain almost unchanged in a long period, indicating that there is no need to execute the retraining operation frequently.

TABLE I
PARAMETER CONFIGURATIONS OF VQ-VAE

B	32	64	96	128	192	256	512	768	1024
D	2	4	8	4	8	16	16	8	16
V	32	32	32	16	16	16	8	4	4

Note: Since the feedback vector \mathbf{q} is actually a set of indices of codewords and \mathcal{R} consists of the real and imaginary components, the parameters satisfy the equation $B = \frac{2K_p N_s L}{V} \log_2 D$.

TABLE II
COMPLEXITY COMPARISON

Hybrid beamforming technique	Complexity
HB-GNN / HC-GNN	$O(GN_{RF}^2(KN_s^2 + N_s N + N^2))$
MLP	$O(GN_{RF}^2(K^2 N_s^2 + KN_s N + N^2))$
MO	$O(IK^2 N_{RF} N_s^2 N^3)$
Method proposed in [7]	$O(DKN^2 \bar{M}^2 \bar{C}^2)$

Note: N and N_{RF} represent the numbers of antennas and RF chains at the BS or the UE, respectively. I represents the number of iterations. D is the number of convolutional layers. \bar{M} and \bar{C} represent the average kernel size and the number of channels in the convolutional network, respectively.

IV. NUMERICAL RESULTS

A. Dataset Description and Simulation Settings

We perform extensive simulations based on the public datasets of DeepMIMO I3 [13]. The data associated with the BS #2 is adopted in the experiment. The downlink carrier frequency and the bandwidth are the 60 GHz band¹ and 100 MHz, respectively. We set $N_t = 64$, $N_{RF,t} = 4$ for the BS and $N_r = 4$, $N_{RF,r} = 2$ for the UE. The number of subchannels K is 128 and there are $N_s = 2$ data streams. The noise power spectral density (PSD) and pilot transmission power are set to be -161 dBm/Hz and 10 dBm, respectively, if not specified otherwise. For pilot transmission, we only use $K_p = 16$ subchannels with $M = 8$, thus $\mathcal{K}_p = \{1, 9, \dots, 121\}$. The pilot length is set to be $L = 16$. The parameter configurations of the proposed VQ-VAE for different feedback overhead B are shown in Table I, where the codebook size and the codeword length are denoted as D and V , respectively. Based on simulation trials, the number of layers of aggregation and combination is set to be $G = 4$ for both HB-GNN and HC-GNN, and the weight factor α is set to be 0.2. We use 60% samples for training, 20% for validation, and 20% for testing.

¹The proposed approach is applicable to a wide range of frequency bands including the centimeter-wave and millimeter-wave bands.

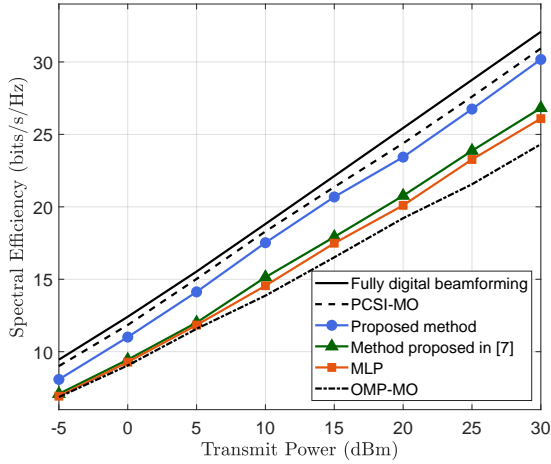


Fig. 3. Spectral efficiency v.s. transmit power

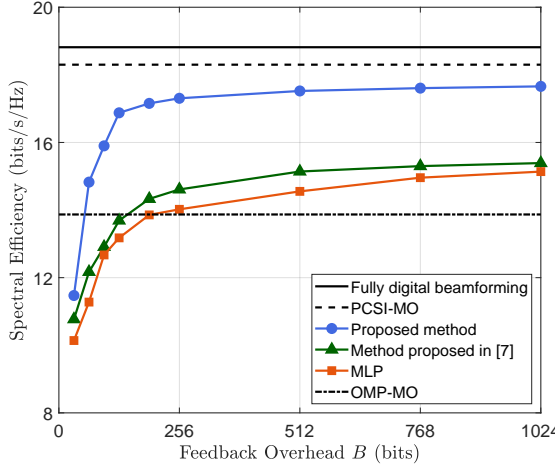


Fig. 4. Spectral efficiency v.s. feedback overhead

B. Performance Evaluation of the Proposed Method

To verify the effectiveness of our proposed method, several benchmarks are selected for comparison, including manifold optimization (MO) with perfect CSI (PCSI), MO with orthogonal matching pursuit (OMP)-based channel estimation, DL method proposed in [7], and the MLP method whose structure has been utilized in many existing works [5], [6], [9]. The fully digital beamforming with PCSI is also considered as a performance upper bound. Here, the MLP method consists of the same structure as the proposed method, but the initialization layer and G aggregation and combination layers in the beamforming network are replaced by $G + 1$ fully-connected layers with an activation function. The DL architecture proposed in [7] primarily comprises convolutional layers and assumes the availability of PCSI at the receiver. An overview of the complexities of different beamforming schemes is presented in Table II.

Fig. 3 shows the average spectral efficiency of proposed method and benchmarks with respect to the transmit power. In the simulation, the feedback overhead is fixed to 512 bits for both the proposed method and MLP method, whereas the other schemes consider infinite-capacity feedback links. It is observed that our method can significantly outperform other methods that require channel estimation, and achieve performance close to the fully digital beamforming (upper bound). The small performance gap between our method and

PCSI-MO may come from the imperfect CSI caused by the limited pilot length, noise to pilot signals, and quantization error in the feedback.

Next, we evaluate the performance of the DL-based methods with different feedback overheads in Fig. 4, where the transmit power is fixed to 10 dBm. It is seen that 256 bits per pilot-bearing subchannel are already sufficient for the proposed method to achieve satisfactory performance. We also observe that the proposed method can outperform MO with OMP-based channel estimation with a feedback overhead of only 64 bits per pilot-bearing subchannel.

V. CONCLUSION

In this paper, we investigate the joint design of pilot, CSI feedback, and hybrid beamforming for the FDD MIMO-OFDM system. A novel DL-based method is proposed, which consists of a PN, an FN, and an HBC-GNN. Therein, the PN uses learned pilot for better CSI acquisition, and the FN via VQ-VAE is designed to improve the feedback efficiency in the limited feedback scenario. Then the HBC-GNN outputs the hybrid beamformer and combiner based on the processed signals at the PN and FN. Simulation results demonstrate the superior performance of our method compared with representative conventional counterparts.

REFERENCES

- [1] W. Chen, X. Lin, J. Lee, A. Toskala, S. Sun, C. F. Chiasserini, and L. Liu, "5G-Advanced toward 6G: Past, present, and future," *IEEE J. Sel. Areas Commun.*, vol. 41, no. 6, pp. 1592–1619, Jun. 2023.
- [2] C.-K. Wen, W.-T. Shih, and S. Jin, "Deep learning for massive MIMO CSI feedback," *IEEE Wireless Commun. Lett.*, vol. 7, no. 5, pp. 748–751, Oct. 2018.
- [3] K. Xu, F.-C. Zheng, P. Cao, H. Xu, X. Zhu, and X. Xiong, "DNN-aided codebook based beamforming for FDD millimeter-wave massive MIMO systems under multipath," *IEEE Trans. Veh. Technol.*, vol. 71, no. 1, pp. 437–452, 2022.
- [4] H. Hojatian, J. Nadal, J.-F. Frigon, and F. Leduc-Primeau, "Unsupervised deep learning for massive MIMO hybrid beamforming," *IEEE Trans. Wireless Commun.*, vol. 20, no. 11, pp. 7086–7099, 2021.
- [5] J. Jang, H. Lee, S. Hwang, H. Ren, and I. Lee, "Deep learning-based limited feedback designs for MIMO systems," *IEEE Commun. Lett.*, vol. 9, no. 4, pp. 558–561, 2020.
- [6] J. Guo, C.-K. Wen, and S. Jin, "Deep learning-based CSI feedback for beamforming in single- and multi-cell massive MIMO systems," *IEEE J. Select. Areas Commun.*, vol. 39, no. 7, pp. 1872–1884, 2021.
- [7] Q. Xue, C. Dong, X. Li, J. Yi, and K. Niu, "Integrated deep implicit CSI feedback and beamforming design for FDD mmwave massive MIMO systems," *IEEE Commun. Lett.*, vol. 12, no. 1, pp. 119–123, 2023.
- [8] K. Wei, J. Xu, W. Xu, N. Wang, and D. Chen, "Distributed neural precoding for hybrid mmwave MIMO communications with limited feedback," *IEEE Commun. Lett.*, vol. 26, no. 7, pp. 1568–1572, 2022.
- [9] F. Sahrabi, K. M. Attiah, and W. Yu, "Deep learning for distributed channel feedback and multiuser precoding in FDD massive MIMO," *IEEE Trans. Wireless Commun.*, vol. 20, no. 7, pp. 4044–4057, Jul. 2021.
- [10] J. Jang, H. Lee, I.-M. Kim, and I. Lee, "Deep learning for multi-user MIMO systems: Joint design of pilot, limited feedback, and precoding," *IEEE Trans. Commun.*, vol. 70, no. 11, pp. 7279–7293, 2022.
- [11] S. Kutty and D. Sen, "Beamforming for millimeter wave communications: An inclusive survey," *IEEE Commun. Surveys Tuts.*, vol. 18, no. 2, pp. 949–973, 4th Quart., 2016.
- [12] A. Van Den Oord and O. Vinyals, "Neural discrete representation learning," *Proc. Adv. Neural Inf. Process. Syst.*, vol. 30, 2017.
- [13] A. Alkhateeb, "DeepMIMO: A generic deep learning dataset for millimeter wave and massive MIMO applications," 2019. [Online]. Available: <https://arxiv.org/abs/1902.06435>